Theory of Anomalous Diffusion Impedance of Realistic Fractal Electrode

ARTICLE *in* THE JOURNAL OF PHYSICAL CHEMISTRY C · MARCH 2008

Impact Factor: 4.77 · DOI: 10.1021/jp712066k

3 AUTHORS, INCLUDING:

Rama Kant
University of Delhi
78 PUBLICATIONS **1,436** CITATIONS

THE JOURNAL OF PHYSICAL CHEMISTRY C LETTERS

2008, *112,* 4019−4023
Published on Web 02/27/2008

Theory of Anomalous Diffusion Impedance of Realistic Fractal Electrode

Rama Kant,* Rajesh Kumar, and Vivek K. Yadav

Department of Chemistry, University of Delhi, Delhi 110007, India

Received: December 25, 2007; In Final Form: February 7, 2008

We developed a theory for the anomalous admittance and the constant phase angle behavior of an irregular interface operating under diffusion controlled charge-transfer condition. Interfacial irregularity is modeled as a realistic random fractal, which is characterized as statistically isotropic self-affine fractals on limited length scales. The power spectrum of such a surface fractal is approximated in terms of a power law function for the intermediate wave numbers. This power spectrum has four fractal morphological parameters. They are fractal dimension (D_H), lower (l) and upper (L) cutoff length scales of fractality, and the proportionality factor (μ) related to topothesy or strength of roughness. Theoretical result obtained for the admittance on such realistic fractal electrode is an indispensable step in the quantitative description of role of roughness and is applicable for all frequency regimes. This result can also be simplified to three limiting laws for the admittance or impedance. The anomalous admittance/impedance and an approximately constant phase angle behavior is explained through a limiting law for the intermediate frequencies. The intermediate frequency limiting law is dependent on the fractal dimension as well as on the lower cutoff length and strength of roughness. Finally, these results also offer an explanation for difficulties in classical power-law form for the diffusive impedance with incomplete characterization of exponent with fractal morphological parameters.

I. Introduction

Electrochemical impedance spectroscopy has been widely used for a long time in the field of electrochemistry, e.g., electrodes kinetics, double layer studies, study of mechanisms of interfacial processes, evaluation of parameters like rate constants and double layer capacitance.[1−3] This method is also used extensively in applied systems like batteries, corrosion, bio-electrochemistry, etc. Most of these measurements are strongly influenced due to surface irregularities and are reflected in their response anomalies like: constant phase angle (CPA) or anomalous frequency $(i\omega)^{\beta}$ dependence (ω being the angular frequency). These surface irregularities are best described as fractals[4] over a limited length scales and often possess limited self-affine scaling property.[5−8]

The diffusion of the reactant from a bulk medium toward an interface where the reactant either looses its activity or is transformed into the product is a common problem in the diverse area of science.[5−28] Diffusion-limited processes on such interfaces show anomalous diffusive behavior. Various other realizations of diffusion-limited processes in physical phenomena are spin relaxation,[10] fluorescence quenching,[10] heterogeneous catalysis,[11] enzyme kinetics,[12] heat diffusion,[13] membrane transport,[4,14] etc. Also there is long standing quest in electrochemistry[5−8,14−32] to understand the effect of interfacial irregularity on the electrochemical response. Two cases in frequency domain have drawn lots of attention to understand anomalous behavior in them. These problems are (i) the capacitive behavior of rough/porous electrodes[23−25,28−32] and (ii) diffusion-controlled (facile) charge transfer on the rough/porous interface.[5−8,16−25] Theoretical understanding of these phenomena offer several open ended questions. Particularly, in the case of realistic surface roughness with limited length scale of irregularities. Some of these are frequently characterized as self-affine fractals[33−35] and a search for the impedance of such electrodes is almost synonymous with finding the response of a random surface profile electrode, and hence is a theoretically challenging problem.

The well-known Warburg admittance of planar electrode[9] is given as

$$Y_W(\omega) = A_0\Gamma(i\omega D)^{1/2} \tag{1}$$

where A_0 is the projected area of the surface, Γ is specific diffusion capacitance, it is defined as $\Gamma = n^2F^2/[RT(1/C_O^0 + 1/C_R^0)]$, $i = \sqrt{-1}$, ω is the angular frequency, D is the diffusion coefficient, n being the number of electron transferred, F is Faraday constant, R is gas constant, T is the temperature; C_O^0 and C_R^0 are bulk concentration of oxidized and reduced species, respectively. Warburg admittance implies that the diffusion-limited admittance is directly proportional to the size of electrode, specific capacitance and the complex depletion layer thickness. This result is applicable for the liquid metal or single-crystal electrode but the presence of geometric disorder (roughness) at the interface makes it realistic but theoretically difficult problem.

The total admittance, $Y(\omega)$, of an interfacial redox reaction, $O + ne^- \rightleftharpoons R$, driven by sinusoidal interfacial potential ($\delta\eta = E - E_e = \eta_0 e^{i\omega t}$, where the equilibrium potential is E_e, here η_0 is the magnitude of applied sinusoidal potential) can be obtained by solving appropriate diffusion equation. The concentration

* To whom correspondence should be addressed. URL: http://people.du.ac.in/~rkant. E-mail: rkant@chemistry.du.ac.in.

10.1021/jp712066k CCC: $40.75

varies locally from C_α^o as $C_\alpha^o + \delta C_\alpha$. The concentration profile of the form $\delta C_\alpha(\vec{r})e^{i\omega t}$, satisfies the diffusion equation in the linear regime

$$i\omega\delta C_\alpha(\vec{r}) = D_\alpha \nabla^2 \delta C_\alpha(\vec{r}) \tag{2}$$

where $\alpha \equiv$ O or R, represents the oxidized or reduced species, D_α is the bulk molecular diffusion constant of species α, δC_α is the difference between surface and bulk concentration and $\vec{r}$ is the three-dimensional vector, $\vec{r} \equiv (x,y,z)$. The linearized boundary condition under Nernstian constraint can be written as

$$\delta C_S(z = \zeta(x,y)) = -nf\eta_0 \Big/ \left(\frac{1}{C_O^0} + \frac{1}{C_R^0}\right) \tag{3}$$

where $\delta C_S(z = \zeta(x,y))$ is the surface concentration and $f = F/RT$. Equation 3 is obtained for $D_O = D_R = D$, through the local Nernstian transfer limitation at the interface (ζ). Here at initial time, and far off from the interface an uniform initial and bulk concentration C_α^0 is maintained viz. $C_\alpha(\vec{r}, t = 0) = C_\alpha(z \rightarrow \infty, t) = C_\alpha^0$. This formalism for diffusion process on a realistic random boundary value problem and its application to corrugated self-affine fractal is described in reference.[6] We wish to use this formalism for present work on realistic (isotropic) self-affine fractal roughness because this is most frequent form of roughness encountered in rough electrodes.

The admittance, $Y(\omega)$, in the intermediate frequency domain is experimentally expressed as power law relation

$$Y(\omega) \sim (i\omega)^\beta \tag{4}$$

where the exponent, β, depends upon the interfacial roughness. De Gennes scaling result justify the theoretical validation for eq 4 with $\beta = (D_H - 1)/2$,[10] and generalized form.[36] De Gennes analyzed it for the diffusion- controlled nuclear magnetic relaxation in porous media with fractal dimension D_H.[10] Later similar results discussed for other diffusion controlled situations such as impedance of rough electrode.[17,18] There are some other general results which emphasize the concept of current/impedance for the diffusion-limited transfer at corrugated surface.[5,6,19−22] Palasantzas[37] also used the formalism discussed in ref 6 to study the admittance of self-affine rough electrode but their analysis is limited to high-frequency region. They completely missed the essential intermediate anomalous frequency behavior of this problem. Recently, we have successfully explained potentiostatic current transient on realistic fractal roughness and their experimental validation for nanometers to micrometer scales of roughness.[7,8] Here we present similar approach to generalized Warburg impedance on realistic fractal surface. This analytical model allows one to probe the complete frequency behavior of diffusive impedance of the reacting interface with roughness and to evaluate the simultaneous consequences of fractal dimension and limited length scales of roughness on anomalous behavior (see Figure. 1).

II. Theoretical Model for Random Isotropic Fractal Roughness

The random surfaces for many natural and artificial surfaces are best described as statistically self-affine fractals.[33,34,39] These surfaces remain statistically invariant under the scale transformation: $(x,y,z) \rightarrow (\lambda x, \lambda y, \lambda^H z)$, where H is the roughness (Hurst's) exponent and is related to fractal dimension as $D_H = 3 - H$. The surfaces with limited scales of such invariance

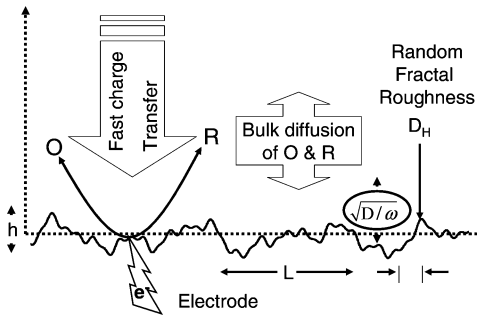

Figure 1. Schematic diagram of a rough working electrode, where a the simple charge-transfer reaction O(sol) + $ne^- \rightleftharpoons$ R(sol) and bulk diffusion of redox species is taking place. The detailed roughness profile is described by a function $z = \zeta(x,y)$, which for random roughness profile is characterized by four roughness parameters viz., the mean square width (h^2) of roughness which is proportional to strength of fractality (μ), lower cutoff length scale (l), upper cutoff length scale (L), and the fractal dimension (D_H).

property can be described by the stationary, Gaussian random processes with a power-law power spectrum over a limited range of wavenumbers.[39] These surfaces also have a power-law mean square height increment function (or the structure function, SF) over a limited (intermediate) length scales is given by[38,39]

$$\langle[\zeta(x,y) - \zeta(x',y')]^2\rangle \approx \tau^{2(1-H)} X^{2H} \tag{5}$$

where $\zeta(x,y)$ is the centered surface profile function, the angular brackets designate ensemble averaging and $X = [(x - x')^2 + (y - y')^2]^{1/2}$. Topothesy ($\tau$)[34,38,39] is defined as the horizontal distance between two points on which SF is equal to τ^2. Topothesy of an 'ideal' fractal surface is related to the normalizing factor (strength) of the power-law spectra (μ) by the following relation:[39] $\tau^{2(1-H)} = 2\,\mu\,\pi\,\Gamma(1 - H)/H\,2^{2H}\,\Gamma(1 + H)$.

The statistically isotropic roughness of the realistic fractal form have four morphological parameters on which the characteristic features of fractal surface are analyzed. The power spectrum of roughness, $\langle|\hat{\zeta}(\mathbf{K})|^2\rangle$, for such a realistic self-affine fractal surface is defined in terms of power law function as

$$\langle|\hat{\zeta}(\mathbf{K})|^2\rangle = \mu|\mathbf{K}|^{2D_H-7}, \text{ for } 1/L \le |\mathbf{K}| \le 1/l \tag{6}$$

where $\hat{\zeta}(\mathbf{K})$ is the Fourier transform (performed over two spatial coordinates, i.e., x and y) of surface roughness profile $\zeta(x,y)$ and $K(= |\mathbf{K}|)$ is the magnitude of wave-vector (K) or simply wave number. The four fractal morphological parameters are: fractal dimension (D_H), lower cutoff length (l) and upper cutoff length L, strength of fractality (μ). As mentioned earlier μ is the strength of fractality, is related to the topothesy of fractals,[34,39] its units are cm^{2D_H-3} and $\mu \rightarrow 0$ means there is no roughness. The lower length scale is the length above which surface shows fractal behavior. Similarly, the upper length scale is the length below which surface shows the fractal behavior. L can also be looked upon as a correlation length above which the height is considered as uncorrelated. It is appropriate to recapitulate that the power spectrum or surface structure factor is (two-dimensional) Fourier transform of two point height−height correlation function of the rough surface. The power spectrum has units of cm^4.

Our general formalism[6] shows that the diffusive admittance/impedance at random rough surfaces can be described in term of its power spectral density of roughness. The main approximation involved in derivation of generalized Warburg equation in reference[6] is the truncation of solution at second order in the

surface roughness profile. The ensemble averaged admittance at the stationary, Gaussian random surface obtained under the diffusion-limited condition is (see eq 13 in ref 6)

$$\langle Y(\omega)\rangle = Y_W(\omega)\left[1 + \frac{1}{(2\pi)^2}\sqrt{\frac{i\omega}{D}}\int \mathrm{d}^2K \times \left(\sqrt{K^2 + \frac{i\omega}{D}} - \sqrt{\frac{i\omega}{D}}\right)\langle|\hat{\xi}(\mathbf{K})|^2\rangle\right] \quad (7)$$

where $\langle Y(\omega)\rangle$ is the ensemble averaged admittance for the rough electrode. d^2K in the integrand represents a double integral over two components of wave-vector with limits $-\infty$ to ∞ and for statistically isotropic surface this simplifies to $\int \mathrm{d}^2K \equiv 2\pi \int_0^\infty \mathrm{d}K\, K$. The generalized Warburg eq 7 for the diffusion limited admittance on randomly rough electrode is proportional to the Warburg admittance on projected surface and a frequency dependent complex dynamic roughness factor. The dynamic roughness factor contains all information about the roughness of the surface through the power spectrum of roughness. The kernel inside the integral depends on the complex diffusion length and picks value of power spectrum at appropriate wavenumbers.

The present theory of anomalous diffusion impedance of realistic fractal electrode is obtained using the solution for the dynamic diffusive admittance on an approximate self-affine surface. Substituting eq 6 for the band-limited power law spectrum in eq 7 and solving resultant integral, we obtained the following equation for total admittance for a band-limited (isotropic) fractal power spectrum as follows:

$$\langle Y(\omega)\rangle = Y_W(\omega)\,[1 + R_I(\omega)] \quad (8)$$

The function, $R_I(\omega)$, is the contribution of roughness in the total admittance and is obtained as

$$R_I(\omega) = \frac{i\omega}{D}\left[\frac{\mu L^{-2\delta}}{4\pi\delta} - \frac{\mu l^{-2\delta}}{4\pi\delta} + \psi(\omega)\right] \quad (9)$$

$$\psi(\omega) = \frac{\mu l^{-2\delta}}{4\pi\delta}\,{}_2F_1\left[\delta, \frac{-1}{2}, \delta + 1, \frac{iD}{l^2\omega}\right] - \frac{\mu L^{-2\delta}}{4\pi\delta}\,{}_2F_1\left[\delta, \frac{-1}{2}, \delta + 1, \frac{iD}{L^2\omega}\right] \quad (10)$$

Here $\delta = D_H - 5/2$ is deviation from the Brownian fractal dimension and ${}_2F_1$ is the hypergeometric function.[40] This admittance expression is dependent on four fractal morphological parameters of roughness and phenomenological diffusion length. Two important limiting frequency behaviors of quantity $R_I(\omega)$ are: (i) $\lim_{\omega\to 0} R_I(\omega) = 0$ and (ii) $\lim_{\omega\to\infty} R_I(\omega) = \mu(l^{-2(\delta+1)} - L^{-2(\delta+1)})/(8\pi(\delta + 1))$. Physically, the first limiting behavior arise from the fact that the diffusion length is much larger than the surface irregularities and the second limiting behavior arise from the fact that the diffusion layer thickness is much smaller than the surface irregularities. These limits imply Warburg admittance like behavior at high and low frequencies.

The anomalous region of admittance for the intermediate frequency can be written in terms of series expansion of two hypergeometric functions in eq 10 viz. one for small $(D/L^2\omega)$ and another for large $(D/l^2\omega)$ and retaining only the leading orders (see appendix for formulas used in these expansions). The admittance equation for the intermediate anomalous region is as follows:

$$\langle Y(\omega)\rangle \approx Y_W(\omega)\left[1 + \frac{i\omega}{D}\left(-\frac{\mu l^{-2\delta}}{4\pi\delta} - \frac{\mu}{8\delta\pi^{3/2}}\Gamma(\delta + 1)\,\Gamma(-\delta - 1/2)\left(\frac{i\omega}{D}\right)^{\delta} + \frac{\mu l^{-2\delta-1}}{4\pi(\delta + 1/2)}\sqrt{\frac{D}{i\omega}} - \frac{\mu l^{-2\delta+1}}{8\pi(1/2 - \delta)}\sqrt{\frac{i\omega}{D}} + \frac{\mu l^{3-2\delta}}{32\pi(3/2 - \delta)}\left(\frac{i\omega}{D}\right)^{3/2}\right)\right] \quad (11)$$

This simplified expression is suitable to obtain anomalous (intermediate) frequency dependence of magnitude and phase angle behavior of admittance/impedance. The variance in admittance in intermediate frequency region is a function of the three fractal morphological parameters say (D_H, l, μ). Equations 8 and 11 extend the conventional representation of the Warburg admittance on smooth surface electrode to the fractally rough electrode. These equations generalize Warburg admittance for a realistic (statistically isotropic) fractal roughness of limited length scales. Equation 11 offers an excellent approximation of eq 8 in all frequency regimes and show some deviation only in very high-frequency limit.

III. Results and Discussion

Here we observe graphically how the roughness influence the magnitude of impedance and how they deviate from the smooth geometry (Warburg) response under the variation of fractal morphological parameters. It shows clearly that the extent of roughness has very significant effect on the magnitude of impedance $|Z(\omega)|$. Nature of the plots shown in Figure 2 elucidates the anomalous scaling behavior in the intermediate frequency regime and its crossover to low and high-frequency Warburg type impedance. Figure 2A shows the effect of fractal dimension (D_H) over the magnitude of impedance for the diffusion-limited charge-transfer process in the frequency domain in logarithmic scale. It is observed that the magnitude of impedance decreases with increase in fractal dimension from top to bottom. In the intermediate frequency domain it shows the approximate power law behavior and merges at lower frequency region with the planar behavior $1/\sqrt{\omega}$. The low frequency outer-cutoff region shifted toward lower frequency domain as the fractal dimension increases. It is also observed that slope of the scaling region does not purely depend upon the fractal dimension but also on lower length cutoff and strength of fractality. In Figure 2B, we observe that the magnitude of impedance increase with increase in the lower cutoff length value. It shows that roughness decreases with the increase in the lower cutoff length scale. Here we are showing the variation of impedance in frequency domain with the variation of lower cutoff length (l) from bottom to top. In this graph we observe that the low frequency outer-cutoff region shifted toward lower frequency domain as the roughness increases. In Figure 2C, we observed that the roughness can also be characterized by the strength of fractality (topothesy), i.e., linearly related to the mean square width (thickness) of the interface. Dependence of slope of the intermediate region on μ is indicate that even under limits: $l \to 0$ and $L \to \infty$, the scaling exponent (β) in eq 4 will be a function of D_H, μ. This is the indication of that sole dependence on β on D_H as perceived in earlier work[10] is an incomplete description. Here the magnitude of impedance deviates from the Warburg response by the variation of μ. The magnitude of generalized Warburg impedance decreases with

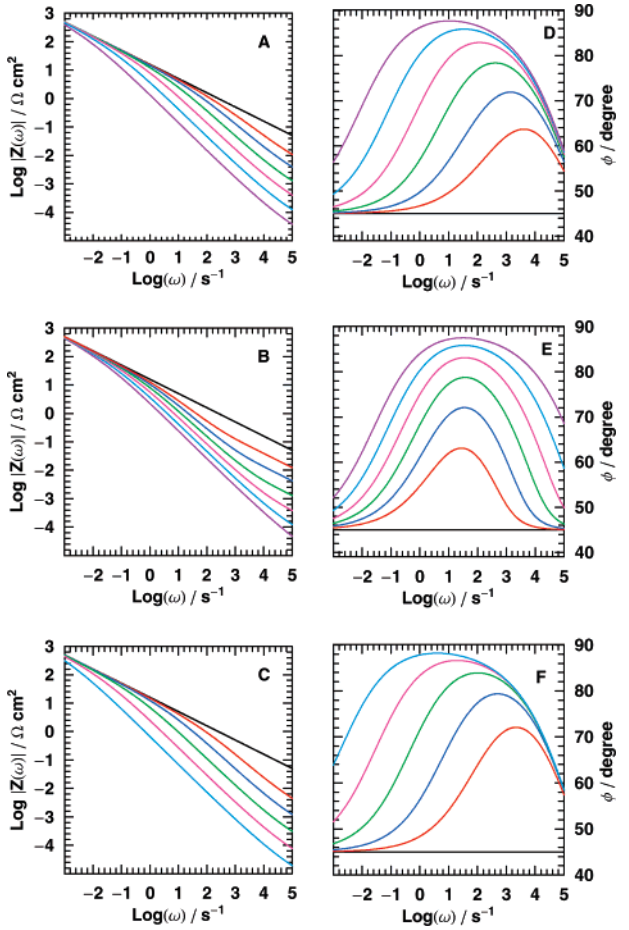

Figure 2. Illustrate the effect of three dominant fractal morphological parameters on Bode plots. The logarithm of magnitude of the impedance $\log(|Z(\omega)|)$ vs the logarithm of angular frequency $\log(\omega)$ (first column of graphs); and the phase angle (ϕ) vs $\log(\omega)$ (second column of graphs) are shown in this figure. The three dominant (fractal) morphological parameters are: (A & D) fractal dimensions (D_H), the parameters were taken as $D_H = 2.2$, 2.25, 2.3, 2.35, 2.45, and $l = 40$ nm, $L = 4$ μm, $\mu = 2 \times 10^{-6}$ a.u., $A = 1$ cm^2, $D = 5 \times 10^{-6}$ cm^2 s^{-1}, and concentration ($C_O = C_R = 15$ mM); (B & E) Lower cutoff length scale (l), the parameters were taken as $D_H = 2.4$, and $l = 20$, 40, 80, 160, 320, and 640 nm and $L = 4$ μm, $\mu = 2 \times 10^{-6}$ a.u., $A = 1$ cm^2, $D = 5 \times 10^{-6}$ cm^2 s^{-1}, and concentration ($C_O = C_R = 15$ mM); (C & F) Strength of fractality (μ), the parameters were taken as $D_H = 2.4$, and $l = 40$ nm and $\mu = (0.05, 0.2, 0.8, 3.2, 12.8) \times 10^{-6}$ a.u., $L = 4$ μm, $A = 1$ cm^2, $D = 5 \times 10^{-6}$ cm^2 s^{-1}, and concentration ($C_O = C_R = 15$ mM); The intermediate frequency domain in these graphs show the anomalous power law behavior and the limited "constant" phase angle (CPA) behavior.

the increase in the value of strength of fractality μ from top to bottom. All the impedance diagrams show the anomalous power law behavior that merges at low frequency.

Remarkable features can be seen in the phase angle plots in Figure 2. In Figure 2D, we observe the effect of fractal dimension over the phase angle response in frequency domain. We can clearly see from the plots that they show the approximately constant phase angle behavior and shifted toward the lower frequency region with the increase in fractal dimension from bottom to top. As the fractal dimension increases, the width of maximum region of phase angle increases. In Figure 2E, we observe the effect of lower cutoff length scale over the phase angle response. The magnitude of the phase angle decreases with the increase in the lower cutoff length value from top to bottom. The width of maxima region of phase angle increases with decreases in the lower cutoff length scale. The "constant" phase angle region is shifted toward the high-frequency region as the lower cutoff length value decreases. In Figure 2F, we observe the influence of strength of fractality (μ) on the nature of phase angle over a frequency range. Here we analyze that the magnitude of phase angle increases with the increase in strength of fractality from bottom to top. From this graph we can see that the "constant" phase angle behavior in the intermediate frequency region and it shifted toward lower frequency region with increase in μ. Hence from all the graphs we conclude that they follow the power law behavior in frequency domain and an approximate CPA behavior in the intermediate region. In general, the magnitude and the width of maxima (CPA) region of phase angle increases with the increase in the roughness factor which increase with the increase in the value of D_H, μ and decrease in l. Our results also show that the lower crossover frequency (ω_o) and the higher crossover frequency (ω_i) of CPA behavior are dependent on all three fractal morphological parameters, i.e., D_H, μ and l. These values differ from what one would naively expect from simple estimates viz. $\omega_o \sim D/L^2$ and $\omega_i \sim D/l^2$. Particularly, this is prominent in ω_o values estimated from graphs. These values show unusually strong extension of CPA toward lower frequencies. This could be due to fact that the power-law power spectrum of roughness implies higher amplitude for long wavelength features of roughness and hence deeper valleys. The transversal diffusion layer is confined to these valleys is perceived shorter than one obtains from the simple physical picture of smooth surface diffusion (or longitudinal diffusion layer). This localization and consequently effective shortening of diffusion layer causes extension of CPA behavior toward lower frequencies.

IV. Conclusion

Here we have analyzed the simultaneous influence of all characteristic roughness parameters on the impedance and the phase angle behavior of rough surface in the frequency domain (using Bode plots). The anomalous scaling behavior in the intermediate frequency regime shows the power law behavior of impedance and the plots are dependent on fractal dimension, lower cutoff length scale and topothesy. Physical reasons for these observations is that at higher frequencies the diffusion length is smaller compared to the surface roughness features and have uniform impedance behavior (characteristic features), whereas in the intermediate region the diffusion length is comparable to the size of surface roughness features, so the roughness features of the surface are reflected in the response of this region. From our graphs we conclude that our theoretical results explain the anomalous power law diffusive frequency dependence and an approximate "constant" phase angle (CPA) behavior in the intermediate frequency domain. We show that the intermediate frequency admittance exponent (β) in eq 4 depend on D_H, l, μ, this is not conceived in earlier work.

The limited length scales fractal surface model led to two important conclusions: (i) the limited scale invariant frequency response is obtained under diffusion-limited transport condition on a limited length scale invariant rough interface and (ii) the scaling exponents of the frequency response is related to the lower length cutoff, strength of fractality and the scaling exponent of the interfacial geometry. Some of the earlier attempts to fractal surfaces are mainly based on idealized fractal model where the direct influence of characteristic roughness parameters like fractal dimension (D_H), strength of fractality (μ), and cutoff lengths (lower cutoff length l and upper cutoff

length L) are never understood simultaneously. Finally one can say, this theory is an indispensable step in the quantitative description of the role of roughness on the Warburg impedance.

Acknowledgment. R.K. thanks University of Delhi for financial support under "Scheme to Strengthen R & D Doctoral Research Programme'' and also thanks referees for their useful suggestions.

Appendix

Useful Expansions. The small z expansion for the hypergeometric function given in the eq 10 is given below:[40]

$$ {}_2F_1(a,b,c,z) = \frac{\Gamma(c)}{\Gamma(a)\Gamma(b)}\sum_{m=0}^{\infty}\frac{\Gamma(a+m)\Gamma(b+m)}{\Gamma(c+m)}\frac{(z)^m}{m!} \qquad (12) $$

The inverse argument expansion for the hypergeometric function given in the eq 10 is given below using ref 40:

$$ {}_2F_1(a,b,c,z) = \frac{\Gamma(c)\Gamma(b-a)}{\Gamma(b)\Gamma(c-a)}(-z)^{-a}\,{}_2F_1 \times \left(a, 1-c+a; 1-b+a; \frac{1}{z}\right) + \frac{\Gamma(c)\Gamma(a-b)}{\Gamma(a)\Gamma(c-b)}(-z)^{-b} \times {}_2F_1\left(b, 1-c+b; 1-a+b; \frac{1}{z}\right) \qquad (13) $$

First part of eq 10 shows large argument value at small value of lower cutoff length scale. Therefore we use eq 13 for converting the expression into inverse argument value at the lower length cutoff scale and after we use eq 12 into that we get eq 11.

References and Notes

(1) Bard, A. J.; Faulkner, L. R. *Electrochemical Methods: Fundamentals and Application*; Wiley: New York, 1980.
(2) Lasia, A. *Modern Aspects of Electrochemistry*, Conway, B. E., et al., Eds.; Kluwer Academic; New York, 1999; No. 32, p 143.
(3) Macdonald, D. D. *Electrochim. Acta* **2006**, *51*, 1376.
(4) Sapoval, B. *Fractal electrodes, fractal membranes and fractal catalyst in Fractals and disordered systems*; Bunde, A., Havlin, S., Eds.; Springer-Verlag: Heidelberg, Germany, 1996.
(5) Kant, R. *J. Phys. Chem. B* **1997**, *101*, 3781.
(6) Kant, R.; Rangarajan, S. K. *J. Electroanal. Chem.* **2003**, *552*, 141.
(7) Kant, R.; Jha, S. K. *J. Phys. Chem. C* **2007**, *111*, 14041.
(8) Jha, S. K.; Sangal, A.; Kant, R. *J. Electroanal. Chem.* **2008**, doi: 10.1016/ j.jelechem. 2007.12.014.
(9) Warburg, E. *Ann. Physik* **1899**, *67*, 493.
(10) De Gennes, P. G. C. R. *Acad. Sci. Paris* **1982**, *295*, 1061.
(11) Pfeifer, P.; Avnir, D.; Farin, D. *J. Stat. Phys.* **1984**, *36*, 699.
(12) Pfeifer, P.; Welz, U.; Wippermann, H. *Chem. Phys. Lett.* **1985**, *113*, 535.
(13) Vandembroucq, D.; Boccaro, A. C.; Roux, S. *Europhys. Lett.* **1995**, *30*, 209.
(14) Gutfraind, R.; Sapoval, B. *J. Phys I France* **1993**, *3*, 1801.
(15) Rangarajan, S. K. *J. Electroanal. Chem.* **1969**, *22*, 89.
(16) Sapoval, B.; Chazalviel, J. N.; Peyriere, J. *Phys. Rev. A* **1988**, *38*, 5867.
(17) Nyikos, L.; Pajkossy, T. *Electrochim. Acta* **1986**, *31*, 1347.
(18) Pajkossy, T.; Nyikos, L. *Electrochim. Acta* **1989**, *34*, 171.
(19) Kant, R. *Phys. Rev. Lett.* **1993**, *70*, 4094.
(20) Kant, R. *J. Phys. Chem.* **1994**, *98*, 1663.
(21) Kant, R.; Rangarajan, S. K. *J. Electroanal. Chem.* **1994**, *368*, 1.
(22) Kant, R.; Rangarajan, S. K. *J. Electroanal. Chem.* **1995**, *396*, 285.
(23) Nyikos, L.; Pajkossy, T. *Electrochim. Acta* **1990**, *35*, 1567 and references therein.
(24) Pajkossy, T. *J. Electroanal. Chem.* **1991**, *300*, 1 and references therein.
(25) De Levie, R. *J. Electroanal. Chem.* **1990**, *281*, 1 and references therein.
(26) Bisquert, J.; Compte, A. *J. Electroanal. Chem.* **2001**, *499*, 112.
(27) Go, J.-Y.; Pyun, S.-I. *J Solid State Electrochem* **2007**, *11*, 323.
(28) Halsey, T. C.; Leibig, M. *Ann. Phys. (NY)* **1992**, *219*, 109; *Europhys. Lett.* **1991**, *14*, 815 and references therein.
(29) Mulder, W. H.; Sluyters, J. H. *Electrochim. Acta* **1988**, *33*, 303.
(30) Ball, R.; Blunt, M. *J. Phys. A : Math. Gen.* **1988**, *21*, 197 and references therein.
(31) Kerner, Z.; Pajkossy, T. *J. Electroanal. Chem.* **1998**, *448*, 139.
(32) Fleig, J.; Maier, J. *Solid State Ionics* **1997**, *94*, 199.
(33) Feder, J. *Fractals*; Plenum: New York 1988.
(34) Sayles, R. S.; Thomas, T. R. *Nature* **1978**, *271*, 431; **1978**, *273*, 573.
(35) William, J. M.; Beebe, T. P., Jr. *J. Phys. Chem.* **1993**, *97*, 6249.
(36) Maritan, A.; Stella, A. L.; Toigo, F. *Phys. Rev. B* **1989**, *40*, 9269.
(37) Palasantzas, G. *Surf. Sci.* **2005**, *582*, 151.
(38) Berry, M. V. *J. Phys. A: Math. Gen.* **1979**, *12*, 781.
(39) Yordanov, O. I.; Atanasov, I. S. *Euro Phys. J. B* **2002**, *29*, 211.
(40) *Handbook of Mathematical Functions*; Abramowitz, M., Stegan, A., Eds.; Dover Publications Inc.: New York, 1972.